Research Article

Journal of PeptideScience

Received: 29 July 2009 Revised: 25 November 2009 Accepted: 27 November 2009 Published online in Wiley Interscience:

(www.interscience.com) DOI 10.1002/psc.1207

Interaction of a β-sheet breaker peptide with lipid membranes

Giuseppe Vitiello,[a,b] Manuela Grimaldi,[c] Anna Ramunno,[c] Ornella Ortona,[a,b] Giovanni De Martino,[c] Anna Maria D'Ursi[c] and Gerardino D'Errico[a,b]*

Aggregation of β-amyloid peptides into senile plaques has been identified as one of the hallmarks of Alzheimer's disease. An attractive therapeutic strategy for Alzheimer's disease is the inhibition of the soluble β-amyloid aggregation using synthetic β-sheet breaker peptides that are capable of binding Aβ but are unable to become part of a β-sheet structure. As the early stages of the Aβ aggregation process are supposed to occur close to the neuronal membrane, it is strategic to define the β-sheet breaker peptide positioning with respect to lipid bilayers. In this work, we have focused on the interaction between the β-sheet breaker peptide acetyl-LPFFD-amide, iAβ5p, and lipid membranes, studied by ESR spectroscopy, using either peptides alternatively labeled at the C- and at the N-terminus or phospholipids spin-labeled in different positions of the acyl chain. Our results show that iAβ5p interacts directly with membranes formed by the zwitterionic phospholipid dioleoyl phosphatidylcholine and this interaction is modulated by inclusion of cholesterol in the lipid bilayer formulation, in terms of both peptide partition coefficient and the solubilization site. In particular, cholesterol decreases the peptide partition coefficient between the membrane and the aqueous medium. Moreover, in the absence of cholesterol, iAβ5p is located between the outer part of the hydrophobic core and the external hydrophilic layer of the membrane, while in the presence of cholesterol it penetrates more deeply into the lipid bilayer.

Keywords: β-amyloid; β-sheet breaker; electron spin resonance; lipid bilayer; spin-label

Introduction

Alzheimer's disease (AD) is by far the most common form of senile dementia, which is estimated to affect up to 35 million individuals worldwide in 2010 [1]. AD is characterized by progressive memory deficit, cognitive impairment and personality changes. The morphological hallmarks found in the brains of AD patients are two types of abnormal protein aggregates [2,3]: neurofibrillary tangles, which occur intracellularly and are composed of paired helical filaments of hyperphosphorylated Tau protein [4] and senile plaques, which occur in the extracellular space and are composed of insoluble β-amyloid peptide (Aβ) aggregates [5].

Aβ is a peptide that is generally composed of 40–42 amino acids, even though shorter (37–39) and longer (43) forms have been also found [6]. It is generated from proteolytic cleavage of the amyloid precursor protein (APP), a type I integral membrane glycoprotein (695–770 residues), by β- and γ-secretases. Aβ is present at a very low concentration ($<10^{-8}$ M) in biological fluids [7], and its physiological role is unknown. In its native form, Aβ is unfolded but aggregates into a β-sheet structure of ordered fibrils under various conditions [8,9]. It was hypothesized that these fibrils may aggregate to form senile plaques. In the past years, amyloid plaques were generally regarded as the cause of cognitive disorder. More recently, the relevance of soluble protofibrillar oligomeric forms of Aβ has been recognized [10]. In particular, it has been shown *in vivo* that the neurotoxic effect of Aβ(1–42) is independent of plaque formation [11] and that protofibrillar intermediates of Aβ induce progressive neurotoxicity in cortical neurons [12].

The mechanism of Aβ fibrillization has not been fully understood. Many studies suggest that lipid membranes have a decisive role in favoring the β-amyloid aggregation [13]. Jarrett and Lansbury suggested that Aβ forms fibrils by the nucleation-dependent polymerization mechanism and lipids could act as heterogeneous seeds for the polymerization [14]. Verdier *et al*. proposed that Aβ–lipid interaction increases the rate of Aβ misfolding/fibrillogenesis, leads to modifications in the bilayer properties and disrupts membrane fluidity and function [15]. For this reason, a particular interest has been developed in Aβ–membrane interactions in order to elucidate the molecular mechanisms of the Aβ-induced cellular dysfunctions underlying the pathogenesis of AD. However, although many studies have been conducted on this subject [16–19], it is still highly controversial.

Comprehension of the Aβ fibrillation mechanism is fundamental to define a therapeutic strategy. In fact, a widely employed approach in the research of anti-Alzheimer agents involves the identification of substances that are able to prevent amyloid aggregation, or to disaggregate the amyloid fibrils through a direct structural interaction with soluble or aggregated peptides. In this regard, a number of small molecules, like Congo red, anthracycline, rifampicin, anionic sulphonates and melatonin, have been reported to interact with Aβ and prevent its aggregation into oligomers and fibrils, reducing toxicity [20–24].

* *Correspondence to: Gerardino D'Errico, Dipartimento di Chimica "Paolo Corradini", Università di Napoli "Federico II" Complesso di Monte S. Angelo, Via Cinthia, I-80126 Napoli, Italy. E-mail: gerardino.derrico@unina.it*

a *Dipartimento di Chimica "Paolo Corradini", Università di Napoli "Federico II" Complesso di Monte S. Angelo, Via Cinthia, I-80126 Napoli, Italy*

b *CSGI (Consorzio per lo Sviluppo dei Sistemi a Grande Interfase), Firenze, Italy*

c *Dipartimento di Scienze Farmaceutiche, Università di Salerno, Fisciano, Italy*

A promising approach employed to make inhibitors of amyloid formation was the design of specific peptides, deriving from Aβ itself, which bind to it and prevent its aggregation. In particular, Tyernberg and coworkers demonstrated that the Aβ hydrophobic domain KLVFF is fundamental for the peptide self-aggregation [25]. They showed that a peptide containing this segment was able to bind to Aβ, thus slackening its assembly into amyloid fibrils. However, the therapeutic usefulness of this peptide is restricted because of its nonnegligible ability to incorporate into amyloid fibrils. Successively, Soto *et al*. claimed that short synthetic peptides, called *β-sheet breakers*, are capable of binding Aβ but are unable to become part of a β-sheet structure [26]. These peptides destabilize the amyloidogenic Aβ conformer and hence preclude amyloid formation. To design β-sheet breakers that specifically bind to the Aβ region implicated in β-sheet formation, these authors focused on the central hydrophobic region within the N-terminal domain of the Aβ protein (amino acids 17–21: LVFFA). Several β-sheet breaker peptides, from 11 to 5 amino acids long with homology to this region, were generated and tested *in vitro* [27]. Proline residues were added in the β-breakers' sequence to disrupt β-sheet formation, as incorporation of this amino acid within a β-pleated structure is highly unfavorable [28–30]. Finally, charged residues were put at the C-terminal part of these peptides to increase solubility.

One of these β-sheet breaker peptides is the iAβ5. This pentapeptide (LPFFD) and its end-protected version, acetylated at the N-terminus and amidated at the C-terminus (Acetyl-LPFFD-amide: iAβ5p), were shown to bind to Aβ with high affinity and to inhibit Aβ misfolding and aggregation [31,32]. Furthermore, it also induced the disassembly of preformed fibrils *in vitro*. The ability of iAβ5 to inhibit peptide self-aggregation and disassembly amyloid fibrils was also demonstrated *in vivo*. The results support the notion that synthetic β-sheet breakers may be useful in stabilizing the normal protein conformation by converting the β-sheet rich conformer back into the normal form [33–35].

In our laboratories, we have focused on the behavior of the Aβ peptide, or its segments, in the presence of lipid bilayers [36] and on the role of β-sheet breaker peptides to disfavor the β-amyloid fibrillization. Here we report an ESR investigation of iAβ5p pentapeptide in the presence of lipid membranes. Owing to the membrane implication in the processes leading to Aβ misfolding and aggregation, information on iAβ5p behavior in the presence of membrane models is strategic for the analyzation of the activity of the β-sheet breaker against Aβ fibrillization in membrane systems.

ESR spectroscopy, by using spin-labeled substances, has proved to be a fruitful experimental approach for the study of the interactions between peripheral as well as integral proteins and membranes. Both the protein, or the polypeptide, and the lipid can be labeled so that the systems can be studied by different 'points of view'. In the present work, we investigate the iAβ5p–membrane interaction by using phospholipids labeled on the acyl chain or, alternatively, peptides labeled at either the C- or the N-terminus.

Materials and Methods

Materials

Dichloromethane and methanol, HPLC-grade solvents, were obtained from Merck (Darmstadt, Germany), while HFIP was obtained from Sigma-Aldrich (St. Louis, MO, USA). The phospholipid dioleoyl phosphatidylcholine (DOPC) was obtained from Avanti Polar Lipids (Birmingham, AL, USA). Cholesterol (CHOL) was obtained from Sigma. Spin-labeled phosphatidylcholines (*n*-PCSL) with the nitroxide group at different positions, *n*, in the *sn*-2 acyl chain were synthesized as described by Marsh and Watts [37,38]. The spin-labels were stored at $-20\,^{\circ}$C in ethanol solutions at a concentration of 1 mg/ml.

Peptide Synthesis

Solid-phase peptide synthesis and purification

The iAβ5p peptide (Ac-L-P-F-F-D-NH_2) was synthesized according to published methods using standard solid-phase synthesis techniques. Protected amino acids and chemicals were purchased from Fluka (Buchs, Switzerland). Fmoc derivatives of amino acids were used in the coupling reactions, and all lateral amino acid protections were TFA labile. The Rink-amide (50–90 mesh, extent of labeling: 0.8–1.0 mmol/g N loading, 1% cross-linked) resin was purchased from Sigma-Aldrich. The amino acid derivatives (fourfold excess) were sequentially coupled to the growing peptide chain by using *O*-(7-azabenzotriazol-1-yl)-1,1,3,3-tetramethyluronium HATU (fourfold excess) in DMF and DIPEA (eightfold excess), and the coupling reaction time was 2 h. After deprotection of the last Fmoc group, the peptide resin was washed with methanol and dried *in vacuo* to yield the protected peptide-Rink-resin. The protected peptide was cleaved from the resin by treatment with TFA/H_2O/phenol/ethanedithiol/thioanisole (reagent K) (82.5 : 5 : 5 : 2.5 : 5 v/v) 10 ml/0.5 g of resin at room temperature for 3 h. After filtration of the exhausted resin, the solvent was concentrated *in vacuo* and the residue was triturated with diethyl ether. The crude peptide was purified by preparative reversed phase HPLC using an assembly column C18 (30 cm, 4 cm, 300 Å, 15 mm spherical particle size column). The column was perfused at a flow rate of 3 ml/min with a mobile phase containing solvent A (water in 0.1% TFA), and a linear gradient from 50 to 90% of solvent B (CH_3CN in 0.1% TFA) in 40 min was adopted for the elution of the peptide. The pure fraction was collected to yield a white powder after lyophilization. The peptide segment was characterized on a Finningan LCQ-Deca ion trap instrument equipped with an electrospray source (LCQ Deca Finnigan, San José. CA, USA). The sample was directly infused in the ESI source by using a syringe pump at the flow rate of 5 µl/min. Data were analysed with Xcalibur software. The sample purity was >98%.

Derivatization of iAβ5p with spin-label MTSL

Spin-label methyl 3-(2,2,5,5-tetramethyl-1-oxypyrrolinyl) methanethiolsulfonate (MTSL), whose molecular formula is shown in Figure 1, was synthesized according to the procedures

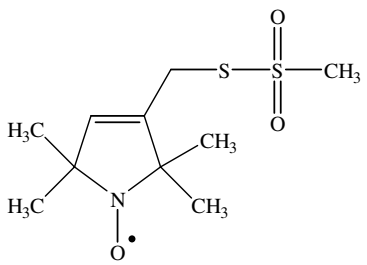

Figure 1. Chemical structure of methyl 3-(2,2,5,5-tetramethyl-1-oxypyrrolinyl) methanethiolsulfonate (MTSL) spin-label.

Journal of PeptideScience

previously reported [39–42]. To insert MTSL on iAβ5p C-terminus and N-terminus, iAβ5p analogs were synthesized including Cys residue at C- and N-terminus respectively, to produce peptides Ac-L-P-F-F-D-C-NH_2 and Ac-C-L-P-F-F-D-NH_2.

The two crude peptides in MeOH/CH_3CN (1 : 1) (4 ml) were incubated with fourfold molar excess of MTSL in acetone (2 ml). The resulting mixture was stirred at room temperature for 72 h. The solvent was removed by filtration and the residue was washed with diethyl ether until no appreciable amount of spin-label MTSL was detected on TLC (ethyl acetate/petroleum ether 65 : 35). The purification of spin-labeled peptides, designated iAβ5p-SL^{C-term} and iAβ5p-SL^{N-term}, respectively, was achieved using a semipreparative RP-HPLC C-18 bonded silica column. The purified peptides were 98% pure as determined by analytical RP-HPLC. Because of the possible reduction of the nitroxide group due to TFA impurity present in the sample, before ESR analysis the peptides iAβ5p-SL^{C-term} or iAβ5p-SL^{N-term} were treated with 10% aqueous ammonia (pH 9.5) for 4 h at room temperature in order to reoxide the spin label back to the nitroxide form [43].

Sample Preparation

Samples of DOPC multi-lamellar vesicles (MLV) were prepared as follows: 20 µg of DOPC, dissolved in a CH_2Cl_2–methanol mixture (2 : 1 v/v, 10 mg/ml lipid concentration), was kept in a round-bottomed test tube, and a thin lipid film was produced by evaporating the solvents with dry nitrogen gas. Final traces of solvents were removed by subjecting the sample to vacuum desiccation for at least 3 h. The samples were then hydrated with 20 µl of 10 mM phosphate buffer at pH = 7.4, gently warmed ($T < 35\,^{\circ}C$), and repeatedly vortexed, obtaining an MLV suspension. The suspension of MLV thus obtained was transferred into a 25-µl glass capillary, and immediately sealed. DOPC vesicles also including CHOL (20% wt/wt on total lipid) were prepared by the same procedure, mixing appropriate amounts of lipid and sterol solutions in CH_2Cl_2–methanol before evaporation of the organic solvents. Similarly, samples containing iAβ5p were prepared by mixing appropriate amounts of the peptide dissolved in HFIP (1 mg/ml) with the lipid organic solutions. For selected samples, we compared results obtained using MLV and unilamellar vesicles obtained by extrusion, and no difference was found. For this reason, all measurements presented below were performed in MLV, which usually leads to more intense and easily detectable ESR signals.

As discussed below, two sets of experiments were performed. In the first one, spin-labeled iAβ5p was used. In this case, the peptide-to-lipid ratio ranged between 4 : 100 and 0.4 : 100 mol/mol. In the second one, PCSL were added to the lipid mixture (1% wt/wt on the total lipid) by mixing appropriate amounts of a spin-label solution in ethanol (1 mg/ml) with the lipid organic mixture. In this case, the peptide-to-lipid ratio was set to 8 : 100 mol/mol.

ESR Spectroscopy

ESR spectra were recorded with a 9-GHz Bruker Elexys E-500 spectrometer (Bruker, Rheinstetten, Germany). Samples were placed in 25-µl glass capillaries and flame sealed. The capillaries were placed in a standard 4-mm quartz sample tube containing light silicone oil for thermal stability. All the measurements were performed at 25 °C. Spectra were recorded using the following instrumental settings: sweep width, 120 G; resolution, 1024 points; time constant, 20.48 ms; modulation frequency, 100 kHz; modulation amplitude, 1.0 G; incident power, 6.37 mW. Several scans, typically 16, were accumulated to improve the signal-to-noise ratio.

Results

Two sets of ESR experiments were performed. In the first one, spin-labeled peptides iAβ5p-SL^{Nterm} or iAβ5p-SL^{Cterm} were dissolved in the appropriate amount of aqueous buffer or liposome solution. Thus, in these experiments the effect of the liposomes on the ESR spectrum of the spin-labeled peptide was observed. In the second set of measurements, spin-labeled phosphocholines, 5-PCSL and 14-PCSL, were inserted in the liposome aggregates at a 1 : 100 spin label/phospholipid mole ratio and the effect of unlabeled iAβ5p peptide on their ESR spectrum was monitored.

The ESR spectra of the two spin-labeled peptides were acquired in phosphate buffer at pH = 7.4, DOPC and DOPC/CHOL (80 : 20 wt/wt) bilayers. In the phosphate buffer, both ESR spectra show the typical lineshape of isotropic fast motion, indicating that the whole molecule is fully exposed to the aqueous medium (see Figure 2a for iAβ5p-SL^{Nterm}).

According to the classical theory of motional narrowing of ESR lines [44], the nuclear spin state dependence of the width of the nitroxide hyperfine line, ΔB, is described by the formula:

$$\Delta B = A + B\,m_I + C\,m_I^2 \qquad (1)$$

where m_I is the nitrogen nuclear spin quantum number. As described in a previous work [45], the values of A, B, and C can be determined by means of a least squares fitting routine of experimental spectra using Eqn (1). In turn, their values allow calculation of the isotropic nitrogen hyperfine coupling constant,

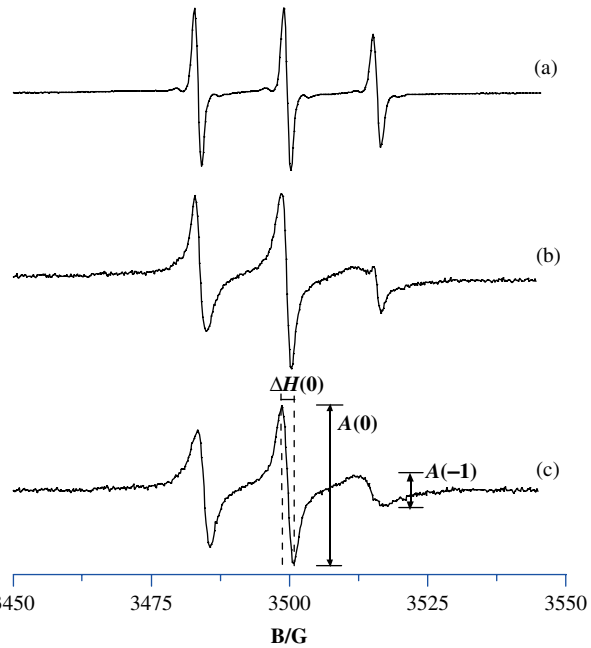

Figure 2. ESR spectra of iAβ5p-SL^{Nterm}: (a) in phosphate buffer, (b) in DOPC membranes (peptide to lipid ratio 1.3 : 100 mol/mol) and (c) slow-motion signal, obtained by subtracting spectrum (a), multiplied by the weighting factor 0.3, from spectrum (b). This figure is available in colour online at www.interscience.wiley.com/journal/jpepsci.

A_N, and the tumbling correlation time of the spin-probe, τ_C. These parameters furnish information about the local physicochemical properties of the label. In particular, A_N depends on the polarity of the medium in which the nitroxide is embedded, whereas τ_C variations clearly show changes in the probe rotational mobility, as determined by the microenvironment viscosity and/or by specific interactions.

For iAβ5p-SL^{Nterm} in phosphate buffer, we found $A_N = 16.13 \pm 0.02$ G and $\tau_C = (5.6 \pm 0.2) \times 10^{-9}$ s. These values are remarkably close to those found for iAβ5p-SL^{Cterm} [$A_N = 16.12 \pm 0.02$ G and $\tau_C = (5.7 \pm 0.3) \times 10^{-9}$ s].

The presence of DOPC liposomes strongly affects the ESR spectra of both spin-labeled peptides. In this case, a complex lineshape characterized by the superposition of two signals is observed (see Figure 2b for iAβ5p-SL^{Nterm}): a fast motion spectrum, similar to that obtained for the peptide in buffer, and a slow-motion spectrum. This evidence indicates that the spin-labeled peptide is distributed in two populations of which the first one is composed by unperturbed molecules dissolved in the aqueous medium, and the second one directly interacts with the phospholipid bilayer. By subtracting the peptide spectrum in buffer from that in DOPC bilayers, we obtained the isotropic slow motion spectrum shown in Figure 2c.

In the case of slow motion spectra, the theory on which Eqn (1) is based does not hold anymore; therefore, we analyzed this spectrum by graphically estimating A_N and τ_C. In particular, the apparent correlation time τ_C was determined according to [46]:

$$\tau_C = (0.65 \times 10^{-9})\, \Delta H_0\, [(A_0/A_{-1})^{1/2} - 1] \qquad (2)$$

where ΔH_0 is the peak-to-peak width of the center line in Gauss, A_0 is the amplitude of the center line and A_{-1} is the amplitude of the high-field line.

For the spectrum reported in Figure 2c, we obtained $A_N = 14.58 \pm 0.02$ G and $\tau_C = (1.9 \pm 0.2) \times 10^{-8}$ s. A decrease in A_N, when compared to that obtained from the spectrum registered in buffer, indicates that the label is embedded in a less polar microenvironment. At the same time, an increase in τ_C indicates that the label motion is hampered. Practically identical results were obtained for iAβ5p-SL^{Cterm} (spectra not shown).

In the presence of DOPC/CHOL bilayers, the ESR spectra of the two spin-labeled peptides show an even more complex lineshape (see Figure 3b for iAβ5p-SL^{Nterm}) given by the overlap of a fast-motion spectrum of unperturbed molecules with an anisotropic slow-motion spectrum. Subtraction of the spectrum in buffer from the experimental one results in the anisotropic spectrum shown in Figure 3c. For anisotropic spectra, evaluation of magnetic and diffusive parameters, analog to A_N and τ_C, is an extremely difficult task. For this reason, analysis of this spectrum was realized determining the outer hyperfine splitting ($2A_{max}$) value. This parameter, obtained by measuring the difference between the low-field maximum and the high-field minimum, through a home-made, MATLAB-based software routine, is dependent on both the amplitude (i.e. order) and rate of chain rotational motion [47], and is therefore a useful parameter for characterizing dynamics of molecules deeply inserted in phospholipid membranes. By analyzing Figure 3c, we found $2A_{max} = 51.7 \pm 0.2$ G. Also, in this case, very similar results were obtained for iAβ5p-SL^{Cterm} (spectra not shown).

ESR spectroscopy allows to quantitatively estimate the partition coefficient of the labeled peptides between the lipid bilayer and the aqueous medium, defined as [48]:

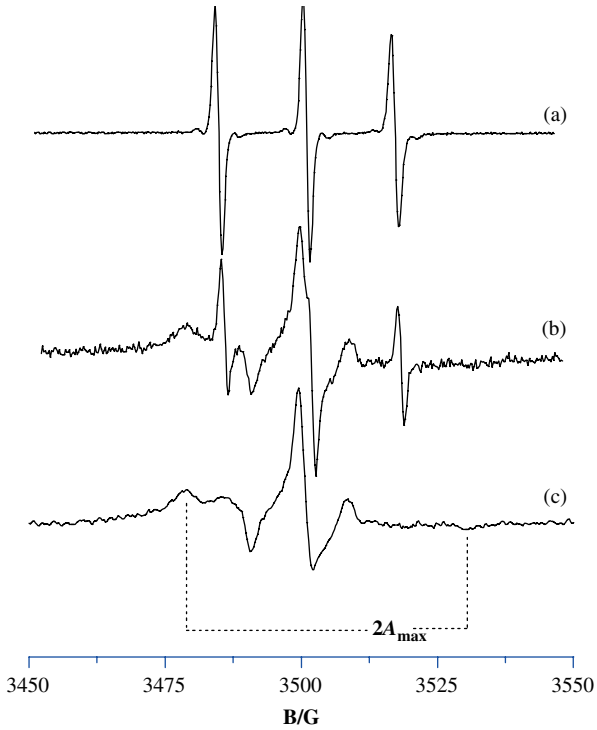

Figure 3. ESR spectra of iAβ5p-SL^{Nterm}: (a) in phosphate buffer, (b) in DOPC/CHOL membranes (peptide to lipid ratio 1.3 : 100 mol/mol) and (c) slow-motion signal, obtained by subtracting spectrum (a), multiplied by the weighting factor 0.6, from spectrum (b). This figure is available in colour online at www.interscience.wiley.com/journal/jpepsci.

$$K_{app} = \frac{X_b}{C_f} \qquad (3)$$

where X_b is the molar fraction of the bound peptide per lipid and C_f is the free peptide concentration. Thus, K_{app} can be determined as the slope of the linear trend obtained by plotting X_b *versus* C_f. Deviations from linearity of this graph indicate either cooperative peptide binding, i.e. strong interactions among the bound peptides, or increasing electrostatic repulsion as the membrane surface becomes charged upon peptide binding [48]. Methodology for obtaining K_{app} from ESR measurements is well established [49]. The fraction of bound peptide, f_b, is calculated according to the relation:

$$f_b = \frac{A(-1)_f - A(-1)_x}{A(-1)_f - A(-1)_b} \qquad (4)$$

where $A(-1)_f$ and $A(-1)_x$ are the peak–peak amplitudes of the high-field ($m_I = -1$) line for the peptide free in solution and in the considered liposomal sample, respectively. $A(-1)_b$ is the amplitude of the high-field line for a fully bound peptide. C_f and C_b, the concentration of membrane-bound peptide, can be calculated from f_b and the known peptide concentration. Finally, X_b can be calculated as the ratio of C_b and the lipid concentration. Application of the method requires various measurements to be conducted at different peptide to lipid ratio.

In Figure 4, the trends of X_b *versus* C_f for iAβ5p-SL^{Nterm} in DOPC and DOPC/CHOL liposomal samples are reported. In both the cases, a linear trend is obtained, i.e. there is evidence of

Journal of PeptideScience

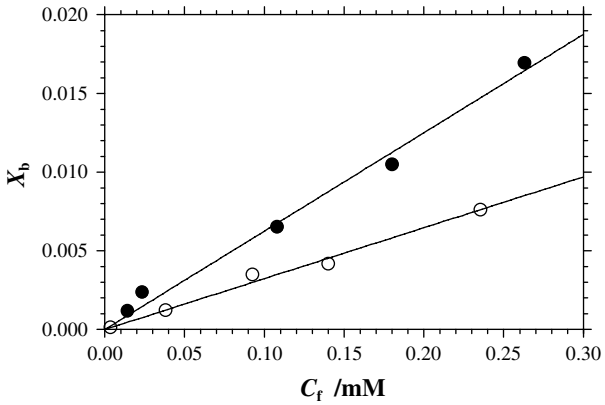

Figure 4. Binding isotherms obtained for iAβ5p-SL^{Nterm} in: DOPC (*full circles*) and DOPC/CHOL bilayers (*open circles*).

Table 1. Outer hyperfine splitting, $2A_{max}$, values of 5-PCSL and 14-PCSL in DOPC and DOPC/CHOL bilayers in the absence and in the presence of iAβ5p

	$2A_{max}$/G
5-PCSL	
DOPC	51.9 ± 0.1
DOPC/iAβ5p	53.3 ± 0.2
DOPC/CHOL	53.5 ± 0.1
DOPC/CHOL/iAβ5p	56.0 ± 0.2
14-PCSL	
DOPC	32.9 ± 0.1
DOPC/iAβ5p	32.7 ± 0.1
DOPC/CHOL	33.7 ± 0.2
DOPC/CHOL/iAβ5p	37.4 ± 0.2

neither cooperativity in peptide binding nor peptide-membrane electrostatic repulsion. The K_{app} values are $62 \pm 2\ M^{-1}$ and $32 \pm 1\ M^{-1}$ for iAβ5p-SL^{Nterm} in DOPC and DOPC/CHOL bilayers, respectively.

As a complementary part of this research, we investigated the interaction between the unlabeled peptide iAβ5p and DOPC or DOPC/CHOL bilayers incorporating PCSL. Analysis of PCSL' spectra was also realized determining the outer hyperfine splitting ($2A_{max}$) values, which are reported in Table 1. The ESR spectrum of 5-PCSL in DOPC bilayers, shown in Figure 5 (lower spectrum, solid line), presents a clearly defined axially anisotropic lineshape, with a value of the outer hyperfine splitting, $2A_{max}$, equal to 51.9 ± 0.1 G. We also investigated DOPC bilayers including phosphatidylcholine spin labeled on the 14 C-atom of the sn-2 chain (14-PCSL), in which the nitroxide group is positioned close to the terminal methyl region of the chain. In this case, a narrow, three-line, quasi-isotropic spectrum is obtained, see Figure 5 (upper spectrum, solid line). The higher isotropy of the 14-PCSL spectrum with respect to that obtained for 5-PCSL indicates a flexibility increase in segmental chain mobility in going from the polar headgroups to the inner hydrophobic core, which is a characteristic hallmark of the liquid-crystalline state of fluid phospholipid bilayers [50].

The association of β-sheet breaker peptide with lipid membranes can be detected by the perturbation of the chain mobility of spin-labeled lipids by using ESR spectroscopy as found for classical water-soluble peripheral membrane proteins and derived

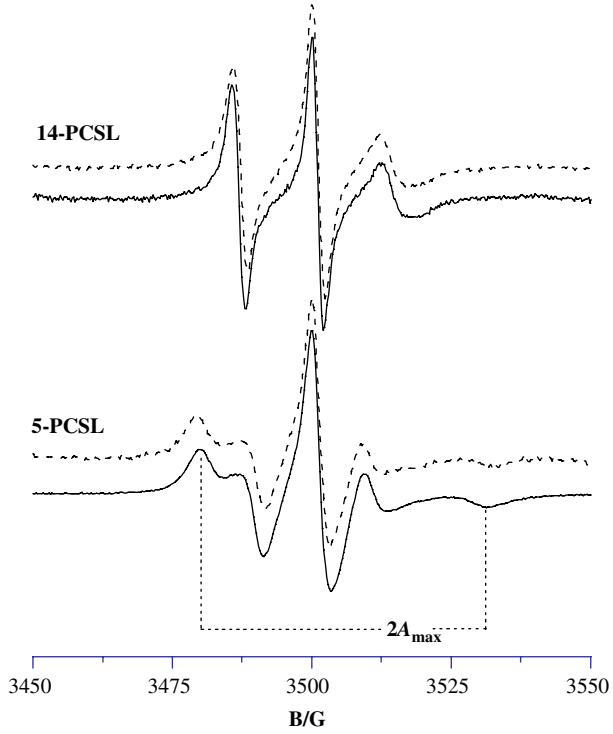

Figure 5. ESR spectra of 5-PCSL and 14-PCSL positional isomers of spin-labeled phosphatidylcholine in DOPC bilayers in the absence (*solid line*) and in the presence (*dashed line*) of 8 : 100 mol/mol iAβ5p peptide. This figure is available in colour online at www.interscience.wiley.com/journal/jpepsci.

peptides [51,52]. Addition of iAβ5p peptide to pure DOPC bilayers, at an 8 : 100 mol/mol ratio, significantly affects the 5-PCSL spectrum, see Figure 5, dashed line. In fact, the peptide causes a slight but significant $2A_{max}$ increase (from 51.9 ± 0.1 to 53.3 ± 0.2 G), i.e. the mobility of the spin-labeled chains decreases by interaction of the peptide with the membrane. In contrast, the addition of iAβ5p to pure DOPC bilayers does not cause any change in the 14-PCSL spectrum, as shown in Figure 5.

We also investigated DOPC bilayers at 20% wt/wt concentration of CHOL, in the absence and in the presence of the peptide. The 5-PCSL and 14-PCSL ESR spectra in DOPC/CHOL bilayers are shown in Figure 6 and the corresponding $2A_{max}$ values are reported in Table 1. Cholesterol induces a $2A_{max}$ increase for both spin-labels. It is interesting to observe that the 14-PCSL spectrum keeps a quasi-isotropic lineshape, an evidence that, despite a certain stiffening, at the considered cholesterol content, the DOPC/CHOL bilayer is still in the liquid disordered state [53].

Addition of peptide at an 8 : 100 mol/mol ratio significantly affects the 5-PCSL spectrum. Indeed, the peptide causes a slight $2A_{max}$ increase (from 53.5 ± 0.1 to 56.0 ± 0.2 G), i.e. the mobility of the spin-labeled chains decreases by interaction of the peptide with the bilayer. The effect of the addition of peptide on the 14-PCSL spectra in DOPC/CHOL bilayers is shown in Figure 6. In this case, a clearly anisotropic spectrum is obtained, as opposed to the quasi-isotropic spectrum obtained in the absence of peptide. This is particularly revealed by the appearence of a second high-field minimum. The $2A_{max}$ trend confirms what is inferred from the spectra. Indeed, the presence of the peptide causes a significant $2A_{max}$ increase with respect to that registered in its absence (from 33.7 ± 0.2 to 37.4 ± 0.2 G), indicating that the peptide is deeply inserted into the lipid bilayer.

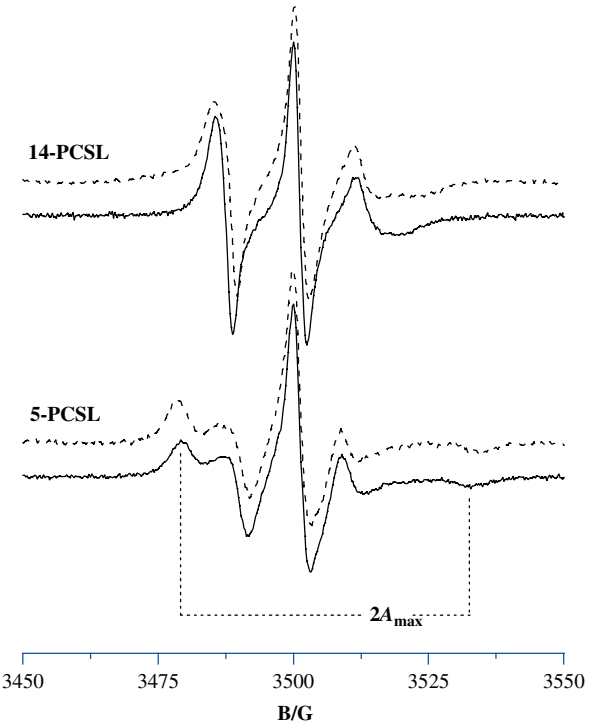

Figure 6. ESR spectra of 5-PCSL and 14-PCSL positional isomers of spin-labeled phosphatidylcholine in DOPC/CHOL bilayers in the absence (*solid line*) and in the presence (*dashed line*) of 8:100 mol/mol iAβ5p peptide. This figure is available in colour online at www.interscience.wiley.com/journal/jpepsci.

Discussion

An attractive therapeutic strategy for AD is to block the early steps of misfolding and aggregation of soluble Aβ peptides using some peptides, named *β-sheet breakers*, which are able to prevent Aβ peptides from assuming β conformation [25,26]. A five-residue synthetic β-sheet breaker peptide, iAβ5, was found to be able to inhibit and disassemble amyloid fibrils *in vitro*. This pentapeptide (LPFFD) is homologous to the central segment of Aβ peptide (amino acids 17–21: LVFFA) and this sequence similarity is important for the specific interaction between β-sheet breaker and Aβ peptides. In particular, the introduction of a proline as a β-sheet blocker residue is fundamental for destabilizing intermolecular β-sheets in Aβ aggregates [54–56]. Moreover, chemical modifications, such as N-terminal acetylation and C-terminal amidation, yield the end-protected peptide, iAβ5p, which presents a major stability and is rapidly taken up by the brain, reducing *in vivo* amyloid deposition [32].

As there is increasing experimental evidence that Aβ peptides self-aggregation occurs close to the cellular membrane surface [13,14], we found of interest to investigate, by spin-label ESR spectroscopy, the interactions between the β-sheet breaker peptide iAβ5p and phospholipid membranes. In the present work, liposomes of the zwitterionic phospholipid DOPC have been initially considered as biomembrane-mimicking systems. In addition, we also considered DOPC bilayers containing CHOL at 20% wt/wt. Indeed, CHOL is a major component of mammalian cells and has been reported to be essential in modulating the interaction of a variety of peptides, including amyloids and lipid bilayers. CHOL is known to influence membrane thickness and fluidity. In turn, the fluidity of the membrane, as modulated by the CHOL content, regulates the insertion of the iAβ5p peptide. At the temperature at which our investigation has been performed (25 °C), the considered membranes are in the fluid-phase state, which may amplify interaction with guest molecules [36,51]. Two sets of ESR experiments were performed. In the first one, spin-labeled iAβ5p analogs containing MTSL as a paramagnetic probe at the N- or the C-terminus of the peptide sequence were used to investigate the peptide interaction with the lipid bilayer. In the second one, we used two spin-labeled phospholipids presenting the nitroxide group in a different position along the hydrophobic alkyl chain to investigate the depth of peptide penetration into the bilayer.

When iAβ5p is in the presence of DOPC membranes, ESR spectra are characterized by superposition of two signals, indicating that the iAβ5p peptide distributes in two populations with different amounts. The presence of the slow component can be attributed to the solubilization of a fraction of peptide molecules in phospholipid bilayer. It is interesting to observe that the ESR signal of interacting peptides does not show any anisotropy. This could suggest a weak interaction of the peptide with the bilayer surface, which leaves the molecule quite free to rotate.

The results also show that the mobility of the spin-labeled peptides is not dependent on the position of the probe MTSL in the peptide sequence. Indeed, iAβ5p-SL^{Nterm} or iAβ5p-SL^{Cterm} present similar ESR spectra in the all considered systems. This evidence suggests no preferential orientation of the peptide in interacting with the bilayer.

In agreement with these experimental evidences, spin-labeled lipids show that peptide molecules insert in DOPC bilayers positioning between the outer part of the hydrophobic core and the external hydrophilic layer. In particular, the results show that the mobility of the spin-label 5-PCSL is significantly affected by the presence of the peptide, while that of 14-PCSL is almost unperturbed.

The presence of CHOL has a significant influence on the iAβ5p/bilayers interaction. When iAβ5p is inserted into the DOPC/CHOL membrane environment, two differently abundant populations result. Peculiarly, the fraction of molecules interacting with the lipid bilayer is characterized by an anisotropic slow-motion spectrum, opposed to the quasi-isotropic spectrum obtained in the absence of CHOL. Furthermore, the presence of CHOL enhances the changes in the 5-PCSL spectrum due to the presence of the peptide. This evidence indicates that the peptide is still able to penetrate the bilayer and that CHOL and peptide exert a synergistic rigidifying action on the bilayer structure. At the same time, in the copresence of CHOL and peptide, the 14-PCSL spectrum shows that the iAβ5p peptide is inserted deeply into the lipid bilayer.

Besides the positioning of the peptide relative to the membrane, ESR spectroscopy allows to quantitatively evaluate the partition coefficient of the peptide between the membrane and the aqueous medium. The obtained K_{app} values, if compared with those reported in the literature for other membrane-interacting peptides [49,57], are quite low. Nevertheless, in consideration of the large excess of binding and/or solubilization sites for peptides offered by the neuronal membrane, our results indicate that, *in vivo*, a significant fraction of iAβ5p is likely to interact with the phospholipid bilayer. Interestingly, inclusion of CHOL decreases the K_{app} value by almost one half. This change, which however is rather modest, suggests that a deep insertion of the peptide involves the rearrangement of the lipid chains.

In conclusion, our experiments show that the β-sheet breaker peptide iAβ5p is partially localized in phospholipid bilayers. In the framework of the model according to which early stages of Aβ peptides self-aggregation occur close to the membrane

Journal of PeptideScience

surface, this β-sheet breaker localization could be strategic for its antiaggregative activity. The membrane fluidity, modulated by the CHOL amount, is critical to drive the positioning of iAβ5p peptide at the membrane interface.

References

1 Prince M, Jackson J. *World Alzheimer Report 2009*. Alzheimer's Disease International: London, 2009.
2 Katzman R, Jackson JE. Alzheimer disease: basic and clinical advances. *J. Am. Geriatr. Soc.* 1991; **39**: 516–525.
3 Selkoe DJ. Alzheimer's disease: genotypes, phenotypes, and treatments. *Science* 1997; **275**: 630–631.
4 Grundke-Iqbal I, Iqbal K, Quinlan M, Tung YC, Zaidi MS, Wisniewski HM. Microtubule-associated protein Tau. A component of Alzheimer paired helical filaments. *J. Biol. Chem.* 1986; **261**: 6084–6089.
5 Hardy JL, Selkoe DJ. The amyloid hypothesis of Alzheimer's disease: progress and problems on the road to therapeutics. *Science* 2002; **297**: 353–356.
6 Murphy MP, Hickman LJ, Eckman CB, Uljon SN, Wang R, Golde TE. γ-secretase, evidence for multiple proteolytic activities and influence of membrane positioning of substrate on generation of amyloid β peptides of varying length. *J. Biol. Chem.* 1999; **274**: 11914–11923.
7 Seubert P, Vigo-Pelfrey C, Esch F, Lee M, Dovey H, Davis D, Sinha S, Schlossmacher M, Whaley J, Swindlehurst C, McCormack R, Wolfer R, Selkoe J, Lieberburg I, Schenk D. Isolation and quantification of soluble Alzheimer's β-peptide from biological fluids. *Nature* 1992; **359**: 325–327.
8 Stine WB, Dahigren KN, Krafft GA, LaDu MJ Jr. In vitro characterization of conditions for amyloid-peptide oligomerization and fibrillogenesis. *J. Biol. Chem.* 2003; **278**: 11612–11622.
9 Vestergaard M, Kerman K, Masato S, Nagatani N, Takamura Y, Tamiya E. A rapid label-free electrochemical detection and kinetic study of Alzheimer's amyloid β aggregation. *J. Am. Chem. Soc.* 2005; **127**: 11892–11893.
10 Mclean CA, Cherny R, Fraser FW, Fuller SJ, Smith MJ, Beyreuther K, Bush AI, Masters CL. Soluble pool of Aβ amyloid as a determinant of severity of neurodegeneration in Alzheimer's disease. *Ann. Neurol.* 1999; **46**: 860–866.
11 Hsia AY, Masliah E, McConlogue L, Yu GQ, Tatsuno G, Hu K, Kholodenko D, Malenka RC, Nicoll RA, Mucke L. Plaque-independent disruption of neural circuits in Alzheimer's disease mouse models. *Proc. Natl. Acad. Sci. USA* 1999; **96**: 3228–3233.
12 Hartley DM, Walsh DM, Ye CP, Diehl T, Vasquez S, Vassilev PM, Teplow DB, Selkoe DJ. Protofibrillar intermediates of amyloid β-protein induce acute electrophysiological changes and progressive neurotoxicity in cortical meurons. *J. Neurosci.* 1999; **19**: 8876–8884.
13 Matsuzaki K. Physicochemical interactions of amyloid β-peptide with lipid bilayers. *Biochim. Biophys. Acta* 2007; **1768**: 1935–1942.
14 Jarrett JT, Lansbury PT. Jr Seeding "one-dimensional crystallization" of amyloid: a pathogenic mechanism in Alzheimer's disease and scrapie? *Cell* 1993; **73**: 1055–1058.
15 Verdier Y, Zarandi M, Botond P. Amyloid β-peptide interactions with neuronal and glial cell plasma membrane: Binding and implications for Alzheimer's disease. *J. Pept. Sci.* 2004; **10**: 229–248.
16 Ambroggio EE, Kim DH, Separovic F, Barrow CJ, Barnham KJ, Bagatolli LA, Fidelio GD. Surface behaviour and lipid interaction of Alzheimer β-amyloid peptide 1–42: a membrane-disrupting peptide. *Biophys. J.* 2005; **88**: 2706–2713.
17 Terzi E, Hölzemann G, Seelig J. Interaction of Alzheimer β-amyloid peptide (1–40) with lipid membranes. *Biochemistry* 1997; **36**: 14845–14852.
18 Bokvist M, Lindström F, Watts A, Gröbner G. Two types of Alzheimer's β-amyloid (1-40) peptide membrane interactions: aggregation preventing transmembrane anchoring versus accelerated surface fibril formation. *J. Mol. Biol.* 2004; **335**: 1039–1049.
19 Lindström F, Bokvist M, Sparrman T, Gröbner G. Association of amyloid-β peptide with membrane surfaces monitored by solid state NMR. *Phys. Chem. Chem. Phys.* 2002; **4**: 5524–5530.
20 Lorenzo A, Yankner BA. β-amyloid neurotoxicity requires fibril formation and is inhibited by Congo red. *Proc. Natl. Acad. Sci. USA* 1994; **91**: 12243–12247.
21 Merlini G, Ascari E, Amboldi N, Bellotti V, Arbustini E, Perfetti V, Ferrari M, Zorzoli I, Marinone MG, Garini P. Interaction of the anthracycline 4′-iodo-4′-deoxydoxorubicin with amyloid fibrils: inhibition of amyloidogenesis. *Proc. Natl. Acad. Sci. USA* 1995; **92**: 2959–2963.
22 Tomiyama T, Shoji A, Kataoka K, Suwa Y, Asano S, Kaneko H, Endo N. Inhibition of amyloid β protein aggregation and neurotoxicity by rifampicin – Its possible function as a hydroxyl radical scavenger. *J. Biol. Chem.* 1996; **271**: 6839–6844.
23 Kisilevsky R, Lemieux LJ, Fraser PE, Kong X, Hultin PG, Szarek WA. Arresting amyloidosis in vivo using small-molecule anionic sulphonates or sulphates: implications for Alzheimer's disease. *Nat. Med.* 1995; **1**: 143–148.
24 Pappolla M, Bozner P, Soto C, Shao H, Robakis NK, Zagorski M, Frangione B, Ghiso J. Inhibition of Alzheimer β-fibrillogenesis by melatonin. *J. Biol. Chem.* 1998; **273**: 7185–7188.
25 Tyernberg LO, Naslund J, Lindqvist F, Johansson J, Karlstrom AR, Thyberg J, Terenius L, Nordstedt C. Arrest of β-amyloid fibril formation by a pentapeptide ligand. *J. Biol. Chem.* 1996; **271**: 8545–8548.
26 Soto C, Sigurdsson EM, Morelli L, Kumar RA, Castano EM, Frangione B. β-Sheet breaker peptides inhibit fibrillogenesis in a rat brain model of amyloidosis: implications for Alzheimer's therapy. *Nat. Med.* 1998; **4**: 822–826.
27 Soto C. Plaque busters: strategies to inhibit amyloid formation in Alzheimer's disease. *Mol. Med. Today* 1999; **5**: 343–350.
28 Chou PY, Fasman GD. Empirical predications of protein conformation. *Annu. Rev. Biochem.* 1978; **47**: 251–276.
29 Kim CA, Berg JM. Thermodynamic β-sheet propensities measured using a zinc-finger host peptide. *Nature* 1993; **362**: 267–270.
30 Wouters MA, Curmi PMG. An analysis of side chain interactions and pair correlations within antiparallel β-sheets: the differences between backbone hydrogen-bonded and nonhydrogen bonded residue pairs. *Protein Sci.* 1994; **3**: 1992–1997.
31 Estrada LD, Soto C. Disrupting β-amyloid aggregation for Alzheimer disease treatment. *Curr. Top. Med. Chem.* 2007; **7**: 115–126.
32 Adessi C, Soto C. Beta-sheet breaker strategy for the treatment of Alzheimer's disease. *Drug Dev. Res.* 2002; **56**: 184–193.
33 Sigurdsson EM, Permanne B, Soto C, Wisniewski T, Frangione B. *In vivo* reversal of amyloid-β lesions in rat brain. *J. Neuropathol. Exp. Neurol.* 2000; **59**: 11–17.
34 Permanne B, Adessi C, Fraga S, Frossard MJ, Saborio GP, Soto C. Are β-sheet breaker peptides dissolving the therapeutic problem of Alzheimer's disease?. *J. Neural Transm. Suppl.* 2002; **62**: 293–301.
35 Permanne B, Adessi C, Saborio GP, Fraga S, Frossard MJ, Van Dorpe J, Dewachter I, Banks WA, Van Leuven F, Soto C. Reduction of amyloid load and cerebral damage in a transgenic mouse model of Alzheimer's disease by treatment with a β-sheet breaker peptide. *FASEB J.* 2002; **16**: 860–862.
36 D'Errico G, Vitiello G, Ortona O, Tedeschi A, Ramunno A, D'Ursi AM. Interaction between Alzheimer's Aβ(25–35) peptide and phospholipid bilayers: The role of cholesterol. *Biochim. Biophys. Acta* 2008; **1778**: 2710–2716.
37 Marsh D, Watts A. Spin-labeling and lipid-protein interactions in membranes. In *Lipid-Protein Interactions*, Vol. 2, Jost PC, Griffith OH (eds). Wiley Interscience: New York, 1982; 53–126.
38 Marsh D. Magnetic resonance of lipids and proteins in membranes. *Curr. Opin. Colloid Interface Sci.* 1997; **2**: 4–14.
39 Powell JH, Johnson EM, Gannett PM. Improvement of a critical intermediate step in the synthesis of a nitroxide-based spin-labeled deoxythymidine analog. *Molecules* 2000; **5**: 1244–1250.
40 Hankovszky HO, Hideg K, Lex L. Synthesis and reactions of highly reactive 1-oxyl-2,2,5,5-tetramethyl-2,5-dihydro-pyrrol-3-ylmethyl sulfonates. *Synthesis* 1980; **11**: 914–916.
41 Mustafi D, Sosa-Peinado A, Gupta V, Gordon DJ, Makinen MW. Structure of spin-labeled methylmethanethiolsulfonate in solution and bound to TEM-1 b-lactamase determined by electron nuclear double resonance spectroscopy. *Biochemistry* 2002; **41**: 797–808.
42 Shafer AM, Kalai T, Liu SQB, Hideg K, Voss JC. Site-specific insertion of spin-labeled L-amino acids in Xenopus Oocytes. *Biochemistry* 2004; **43**: 8470–8482.
43 Karim CB, Zhang Z, Thomas DD. Synthesis of TOAC spin-labeled proteins and reconstitution in lipid membranes. *Nat. Protoc.* 2007; **2**: 42–49.

44 Kivelson D. Theory of ESR linewidths of free radicals. *J. Chem. Phys.* 1960; **33**: 1094–1106.
45 Tedeschi AM, Franco L, Ruzzi M, Paduano L, Corvaja C, D'Errico G. Micellar aggregation of alkyltrimethylammonium bromide surfactants studied by electron paramagnetic resonance of an anionic nitroxide. *Phys. Chem. Chem. Phys.* 2003; **5**: 4204–4209.
46 Bates IR, Boggs JM, Feix JB, Harauz G. Membrane-anchoring and charge effects in the interaction of myelin basic protein with lipid bilayers studied by site-directed spin labeling. *J. Biol. Chem.* 2003; **278**: 29041–29047.
47 Moser M, Marsh D, Meier P, Wassmer KH, Kothe G. Chain configuration and flexibility gradient in phospholipid membranes. Comparison between spin-label electron spin resonance and deuteron nuclear magnetic resonance, and identification of new conformations. *Biophys. J.* 1989; **55**: 111–123.
48 Seelig J. Thermodynamics of lipid-peptide interactions. *Biochim. Biophys. Acta* 2004; **1666**: 40–50.
49 Bhargava K, Feix JB. Membrane binding, structure, and localization of cecropin-mellitin hybrid peptides: a site-directed spin-labeling study. *Biophys. J.* 2004; **86**: 329–336.
50 Swamy MJ, Marsh D. Spin-label electron spin resonance studies on the dynamics of the different phases of N-biotinylphosphatidylethanolamines. *Biochemistry* 1994; **33**: 11656–11663.
51 Ramakrishnan M, Jensen PH, Marsh D. α-Synuclein association with phosphatidylglycerol probed by lipid spin labels. *Biochemistry* 2003; **42**: 12919–12926.
52 D'Errico G, D'Ursi AM, Marsh D. Interaction of a peptide derived from glycoprotein gp36 of feline immunodeficiency virus and its lipoylated analogue with phospholipid membranes. *Biochemistry* 2008; **47**: 5317–5327.
53 Davis JH, Clair JJ, Juhasz J. Phase equilibria in DOPC/DPPC-d62/Cholesterol mixtures. *Biophys. J.* 2009; **96**: 521–539.
54 Moretto V, Crisma M, Bonora GM, Toniolo C, Balaram H, Balaram P. Comparison of the effect of five guest residues on the β-Sheet conformation of Host $(L\text{-Val})_n$ oligopeptides. *Macromolecules* 1989; **22**: 2939–2944.
55 Mutter M, Nefzi A, Sato T, Sun X, Wahl F, Wohr T. Pseudo-prolines (ψ Pro) for accessing ''inaccessible'' peptides. *Pept. Res.* 1995; **8**: 145–153.
56 Wood JS, Wetzel R, Martin JD, Hurle MR. Prolines and amyloidogenicity in fragments of the Alzheimer's peptide β/A4. *Biochemistry* 1995; **34**: 724–730.
57 Pistolesi S, Pogni R, Feix JB. Membrane insertion and bilayer perturbation by antimicrobial peptide CM15. *Biophys. J.* 2007; **93**: 1651–1660.

